SAYAM Vol-I, Issue-I (June, 2023), Page No-01-08

Journal Homepage: https://sayamjournal.com/

Article

Recent advances in the synthesis and biomedical applications of α-hematite nanoparticles

Saheli Ghosh[a], Dhananjoy Mondal[a], Shubham Roy[a], Sukhen Das[a*]

[a] Department of Physics, Jadavpur University, Kolkata-700032, India

[*] Corresponding author email id: sdasphysics@gmail.com

ARTICLE INFO

Keywords:
Biomedical Applications,
Magnetic Nanoparticles,
Hematite,
Nanoparticles .

Received : 28/08/2022
Accepted : 28/04/2023
Date of Publication: 02/06/2023

ABSTRACT

Iron oxide is a chemical compound of iron and oxygen having different polymorphs including Fe_2O_3, Fe_3O_4, and FeO. Among them, most studies were carried out on Fe_2O_3 and Fe_3O_4, as they possess extraordinary properties at the nanoscale. The Fe_2O_3 also has different forms i.e ferrimagnetic γ-Fe_2O_3 (maghemite), weak-ferromagnetic and hard-magnetic ε-Fe_2O_3. In this short review, we have dealt with the α- Fe_2O_3 (hematite) nanoparticles and their biomedical aspects. The high aspect ratio of the particles in the nano-domain enhances its optical, electrical, and magnetic properties. Therefore, in the nano regime, these materials become favorable for various applications such as drug delivery, separation, magnetic hyperthermia, magnetic sorting, sensing, etc. In this report, numerous synthesis protocols (both chemical and physical) of the hematite have been discussed with their potential application in biomedical fields.

INTRODUCTION

In recent times, researchers are paying great attention to synthesizing nanoparticles. Research and investigation on nanoparticles expose a wide area of the invention in science and technology. Synthesizing nanoparticles and studying their properties spread out various scopes to excel in various fields. As these nanoparticles are having excellent physicochemical properties elucidating lots of applications starting from the field of electronics to biology, researchers are interested in studying their characteristics. Although chemically synthesized nanoparticles are gaining importance, they might have the issue of cost-effectiveness, and negative impact on biota from toxicity (Mishra and Singh 2015; Vurro et al. 2019; Banu et al. 2021). Thus, scientists are focusing on the application of natural materials as they are eco-friendly, biocompatible, and also available adequately in our environment (Muhammadi et al. 2015; Kim et al. 2017; Soufi and Iravani 2020). Hence, it is convenient to choose a material that is abundant in nature and has low toxicity. The priority is also given to making low-cost, easily accessible devices like electronic and solid-state devices that could become the future. Hematite (α-Fe_2O_3) is one of such common materials accessible in the environment (Rosso et al. 2010; Dehner et al. 2011; Sharma et al. 2019; Al-Hakkani et al. 2021). Ample amounts of hematite are found in nature, which is non-toxic as well as biocompatible. It has excellent electrical, optical, and magnetic properties. These properties can be utilized to apply in different domains. Hematite nanoparticles have hordes of application fields like biomedical applications, electronic applications, sensing applications, etc. In this review, different methods of synthesizing hematite and its application in the biomedical field will be discussed in a broad spectrum.

SYNTHESIS OF HEMATITE NANOSTRUCTURES

There are several methods to synthesize hematite nanoparticles. It can be classified as top-down and bottom-up approaches and these are depicted.

Bottom-up synthesis protocols

Electrochemical anodization

There are lots of bottom-up approaches for synthesizing hematite (α-Fe_2O_3) nanoparticles among which this method is generally used for the production α-Fe_2O_3 in large amounts. Momeni et al. synthesized α-Fe_2O_3 using ethylene glycol (EG), NH_4F (Ammonium fluoride) as electrolytes, iron foil as an anode, and platinum foil by means of the cathode. The microstructure of the synthesis hematite is a nanotube structure and the size of this varies (39-43 nm) with the reaction time. The band gap has been found to have a value of 2.03 eV in this case. It is observed that some pores can be produced or created by the electrochemical synthesis method which is tuned by varying anodizing durations. The developments of photo-electrochemical and optical properties have also been noticed in this regard (Momeni et al. 2015).

M. M. Momeni et. al. (2015) utilized 1mm thickness Iron foil (99.9% pure) cut it into 10X10 mm coupons and mounted it using resin. Then emery papers of grades 80, 320, 800,1200, and 2400 were used for polishing electrodes and electrodes were washed with distilled water and ethanol. Thereafter, it was rinsed with distilled water. Using the two-electrode system with platinum foil as the cathode and iron foil as the anode and ethylene glycol containing 1M H_2O (pH=11) as an electrolyte, the anodization experiments were performed. The DC voltage was 40V at 25°C for 60 min. The conductivity of the solution was 0.71mS cm^{-1}. Then the samples were annealed for converting amorphous to crystalline Fe_2O_3 in an oxygen atmosphere for 1hr at 450 °C (2°C min^{-1}).

Sol-gel synthesis route

It is also an important technique to form α-Fe_2O_3 nanoparticles. Tadic et al. (2021) used tetraethyl orthosilicate (TEOS), ethanol, and $Fe(NO_3)_3$ to produce hematite nanoparticles by the sol-gel method (**Fig. 1**). Herein, the particle size changes depending on several reaction parameters and it also enhances the magnetic properties of the material radically. The reaction duration greatly affected the size of the nanoparticles (10-20 nm) (Tadic et al. 2021).

Paulson and Jothibas (2021) used 0.3M of $FeCl_3$ (anhydrous Ferric Chloride) and dissolved it in the 100ml distilled water for min with a 300 rpm stirring rate. After that, 10ml NH_3 (ammonia) solution and 10ml distilled water were added together for the preparation of 1:1 reagent solution. Then this solution was poured into the solution of $FeCl_3$ under vigorous stirring 400 rpm for 1hr at 80°C which produced "brownish-yellow" colored gel suspension. Thereafter, the solution was centrifuged by repeated washing with distilled water for 20 mins at 3500 rpm. After this, the gel solution was moved into the Petri plate and dried at 80°C for 24 hrs in an oven. Finally, the powder sample was calcinated under an air atmosphere for 3hrs at 400°C.

Electrospinning method

Electrospinning is one of the important methods to synthesize one-dimensional α-Fe_2O_3. PVP (Polyvinylpyrrolidone) and iron acetate, FeAc2 nanofiber have been used to fabricate α-Fe_2O_3 nanotubes by Eid et al. Herein, the morphology has been controlled by altering the precursor weight ratios of $Fe(NO_3)_3$ and PVP. The synthesized nanoparticles are formed in this way and have outstanding gas-sensing properties (Eid et. al. 2011).

Eid et. al. (2010) has prepared a 7% PVP (polyvinyl pyrrolidone) solution with ethanol. Iron acetate was dissolved in 1ml acetic acid and mixed with a polymer solution of 7ml for synthesizing Fe_2O_3 nanofibers using electrospinning and atomic layer deposition methods. After stirring of the solution for 4hrs, it was squeezed out through the nozzle on which voltage was applied. Due to the applying electrostatic forces, the solution was accelerated onto the surface of the target forming the nanofibers. Then two techniques were used for annealing the collected nanofibers PVP/$FeAc_2$ which were i) in hydrogen atmosphere (95% Ar, 5% H_2) for 4 h at 350°C with a rate of heating around 3°C min^{-1} and ii) in the air with a rate 5°C min^{-1} by varying temperature from room temperature to 550°C; and the cooling rate at room temperature for 12hrs.

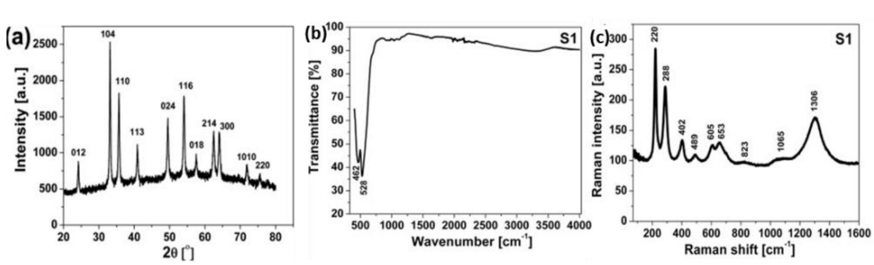

Figure 1 a) X-ray diffractogram, b) Raman spectrum, c) FTIR spectroscopy, (Trpkov et al. 2018)

Hydrothermal method

One of the most common and easiest ways to synthesize α-Fe_2O_3 nanoparticles is the hydrothermal/solvothermal approach. It usually impacts the nanocrystalline structures of the material. Zhu et al. have grown hematite nanoparticles hydrothermally using $FeCl_3$ PVP (Polyvinylpyrrolidone) and NaAc in deionized water (Zhu et al. 2012). The entire procedure has been controlled by adjusting the amount of the reagents and reaction time, which implies that the particle size varies significantly with time. Different types of morphologies like nanorod, nanowire, and also spherical shapes have been grown by this process by varying the reaction parameters such as time, temperature, and pH. Electrochemical, electrical, and magnetic properties can be developed in hydrothermally synthesized nanoparticles (**Fig. 3**).

Zhu et al. (2012) employed a hydrothermal method for synthesizing of hematite nanoparticles using 4 mmol $FeCl_3 \cdot 6H_2O$, 1.0 g of PVP, and 40 mmol NaAc dissolving into 30ml distilled water at 40°C for 2hrs. After that, the solution had been shifted into a "Teflon-lined stainless-steel autoclave" and heated for 18 hrs at 200°C. Then it was cooled and centrifuged using distilled water as well as ethanol for three times. The obtained products were dried at 70°C for 12 hrs under a vacuum.

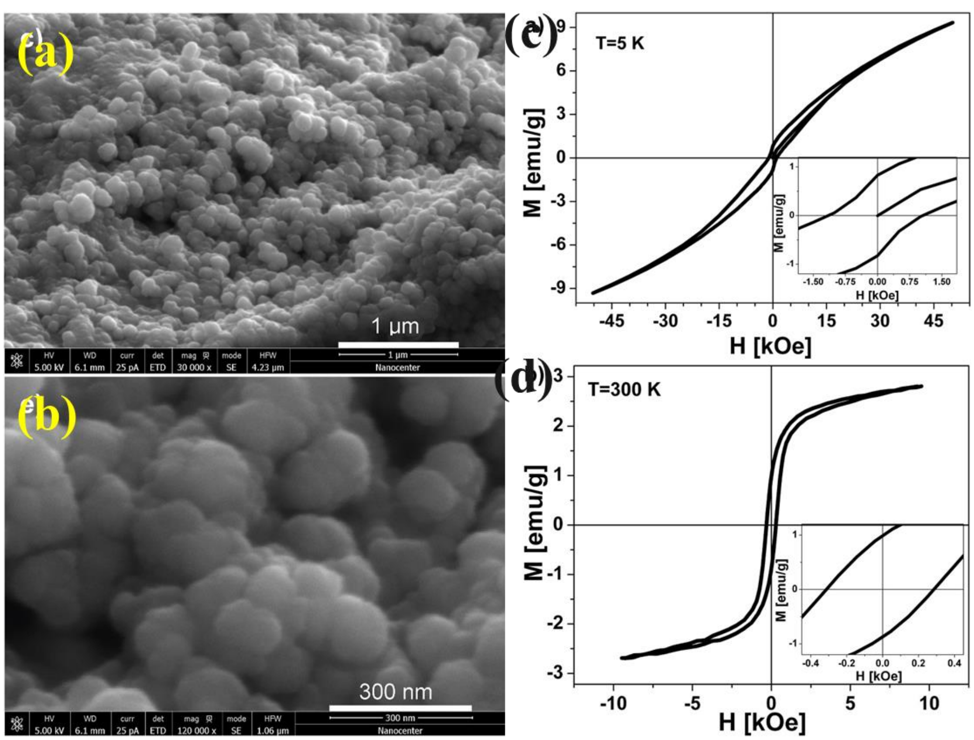

Figure 2 a)- b) Field emission scanning electron microscopy (FESEM) of Hematite NPs, c) Magnetic M-H loop of hematite at 5K temperature, d) Magnetic M-H loop of hematite at 300K temperature (Tadic et al. 2022).

Top to bottom synthesis method

The high-energy ball-milling is one of the top-down synthesis approaches to achieve α-Fe_2O_3 nanoparticles by crushing the natural hematite (bulk) in a ball mill grinder. Ghosh et al. offered a significant contribution in synthesizing purely natural α-Fe_2O_3 nanoparticles by adopting this unique approach to fabricate natural energy harvesting devices. They obtained the nanoform of α-Fe_2O_3 by ball-milling the bulk hematite for 9 hrs with maintaining the ball-to-sample mass ratio 20:1 at 300 rpm. Thus, it can be a promising green alternative to get hematite nanoparticles in a sustainable way. It is interesting to observe that the particle size and the morphology vary significantly with the ball milling duration and it also improves the purity as well as electrical properties of the nanoparticles by enhancing the aspect ratio of the sample (Ghosh et al. 2021). They have found that the electrical properties enhanced with decreasing particle size and gained maximum value in the nano dimension for its maximum surface-to-volume ratio.

Table 1 Different synthesis protocols of hematite NPs

Synthesis Method	**Reagents**	**Morphology**	**Reference**
Electrochemical anodization	Ethylene glycol (EG) and NH_4F as electrolytes, Iron foil as anode and platinum foil as cathode	Nanotube	11
Sol-gel Method	Orthosilicate (TEOS), ethanol, $Fe(NO_3)_3$	Rhombohedron	13
Electrospinning method	PVP (Polyvinylpirrolidon) and iron acetate nanofibre	Nanotube	15
Hydrothermal method	Propane diamine and $FeCl_3$	Nanorod	18
Ball Milling Method (Top Down method)	Natural Hematite (Bulk)	Hexagonal	20

SEVERAL PARAMETERS DEPENDENT PHYSICOCHEMICAL PROPERTIES OF HEMATITE

The shape, size, and microstructure of nanoparticles play a vital role in altering the properties of the materials. The properties as well as the performance of the hematite nanoparticles not only depend on the chemical composition, but also the morphology and inherent microstructure of the hematite. Wang et. al. (2008) and Liu et.al (2012) have established that morphology, size, and porosity are important factors for photocatalytic activities. The shape of the nanoparticles also has a great part in the improvement of characteristics. Since it is well known that the shape and size, in addition to other physical and chemical parameters, also affect the characteristics of inorganic materials, various researchers have thus obtained different controllable sizes and shapes, such as nanorods, nanotubes, nano drums, etc., for further modification of the properties as well as application purpose. Liu et. al. (2010) synthesized hematite of different morphologies which affects the properties of the materials like high-field remanence. In the case of pseudocubic samples the remanence decreases gradually due to cooling and is stable under 60K because of remanence memory and initial IRM has been demagnetized after a complete LTC cycle. In the case of rhombohedral and platy samples, 50% of the remanence has been demagnetized. Again, At 300 K, pseudocubic samples have lower magnetization but larger coercivity than the rhombohedral samples and platy.

Chen et. al. (2014) investigated that the band gap varies with the microstructure of the sample. They have observed that the approximate values of the direct and indirect band gaps of nanorods, nanoparticles, and nanotubes were found 1.90, 1.89, 2.1 eV, and 1.72,1.56,1.78 eV respectively.

In the case of nanoparticles, higher amount of reaction sites and excited states are available as these have higher surface area than the surface area of nanorods and nanoparticles. Thus, hematite nanoparticles exhibits better photocatalytic activity than nanorods and nanotubes. The rate constants (k′) of the nanoparticles, nanotubes, and nanorods, were 0.0064, 0.005, 0.0049 min^{-1} (Chen and Lin 2014).

Hematite in nanoforms has better electrochemical properties than the bulk of the same materials. Zhao et. al. (2015) explored that the nanospindels nanostructure shows better stability in electrochemical performance as the decrease in the capacity rate of these spindle-like structures is lower after 10 cycles than that of nanoplates and nano drums structures. Although the initial discharge–charge capacities of nanoplates, nano spindles, nano drums are 1322/ 977, 1274/858, and 1455/970 mA h g-1 respectively measured when the current density is 0.1 mA cm-2.

The Specific capacitance values for hematite (polyhedral) nanoparticles (40 nm) and hematite (1 μm) are 340.5 F·g−170.8 F·g−1 at the current density of 1 A·g^{-1}. Thus not only the shape but also the size affects the electrochemical properties of the material (Zhu et al. 2012). Even after 500 cycles the retention of capacitive nature is well maintained in the case of hematite nanoparticles.

Zhao et. al. (2015) synthesized different morphological hematite using the hydrothermal method by heating at 200 for 30 hrs.

Table 2 Morphology dependent capacity variance

$NH_3.H_2O$/ml	EG/ml	Morphology	Capacitances (mA h g^{-1})
7	13	Nanoplates	1322
10	10	Nanodrums	1455
15	5	Nanospindles	1274

Chen et. al. (2014) has developed different morphology-dependent photo-catalytic activity varying in several conditions mentioned in the table below:

Table 3 Synthesis dependent variance of morphology and magnetisation

Materials	Time	Temperature (°C)	Morphology	Rate constant of photocatalytic activity (min^{-1})	Magnetisation (Oe)
0.046 M $Fe(NO_3)_3 \cdot 9H_2O$ solution and a 0.002 M $NaH_2PO_4 \cdot 2H_2O$	48 hrs	220	Nanoparticles	0.0064	800
0.02 M $FeCl_3$ and 7.4 × 10−4 M $NH_4H_2PO_4$	6 hrs	220	Nanorods	0.0049	535
0.02 M FeCl3 and 7.4 × 10−4 M $NH_4H_2PO_4$	48 hrs	220	Nanotubes	0.005	348

APPLICATION OF A-HEMATITE IN BIOMEDICAL FIELDS

Nanoscale science and technology deals with the fundamental levels of a particular matter i.e the atomic and molecular levels. Precisely, nanoparticles are gaining attention due to their high aspect ratio which makes the material suitable for showing reasonable efficacy in numerous fundamental properties (Dena et al. 2022; Dahl et al. 2007; Gutfleisch et al. 2011). In this report, the different applications of α-Hematite have been discussed in its nano regime.

Because of their size, nanoparticles (NPs) are perfect for creating functional nanostructures and nano-engendering their surfaces. (Gutfleisch et al. 2011; Smith et al. 2012; Strano et al. 2019). Among other biological applications, these nanoparticles can be altered for use in targeted drug administration, magnetic resonance imaging (MRI), and cancer therapy. (Ma et al. 2012; Li et al. 2014; Nakamura et al. 2015; Liu et al. 2021).

Tadic et al. (2020) investigated the magnetic property of hydrothermally synthesized different morphological hematite and its magnetic resonance imaging (MRI) modalities. They have synthesized two different morphologies (rhombohedron and plate-like) of hematite. The α-hematite rhombohedron showed a hysteresis loop with a coercivity of 22 Oe at room temperature whereas the plate-like hematite showed 24 times higher (522 Oe) coercivity. The transverse relaxivity rates (r2) have been estimated on 15.2 T magnetic resonance imaging (MRI) and showed that rhombohedrons and plate-like hematite exhibited 10.72 and 12.63 mM^{-1} S^{-1} respectively (**Fig. 3**) (Tadic et al. 2021).

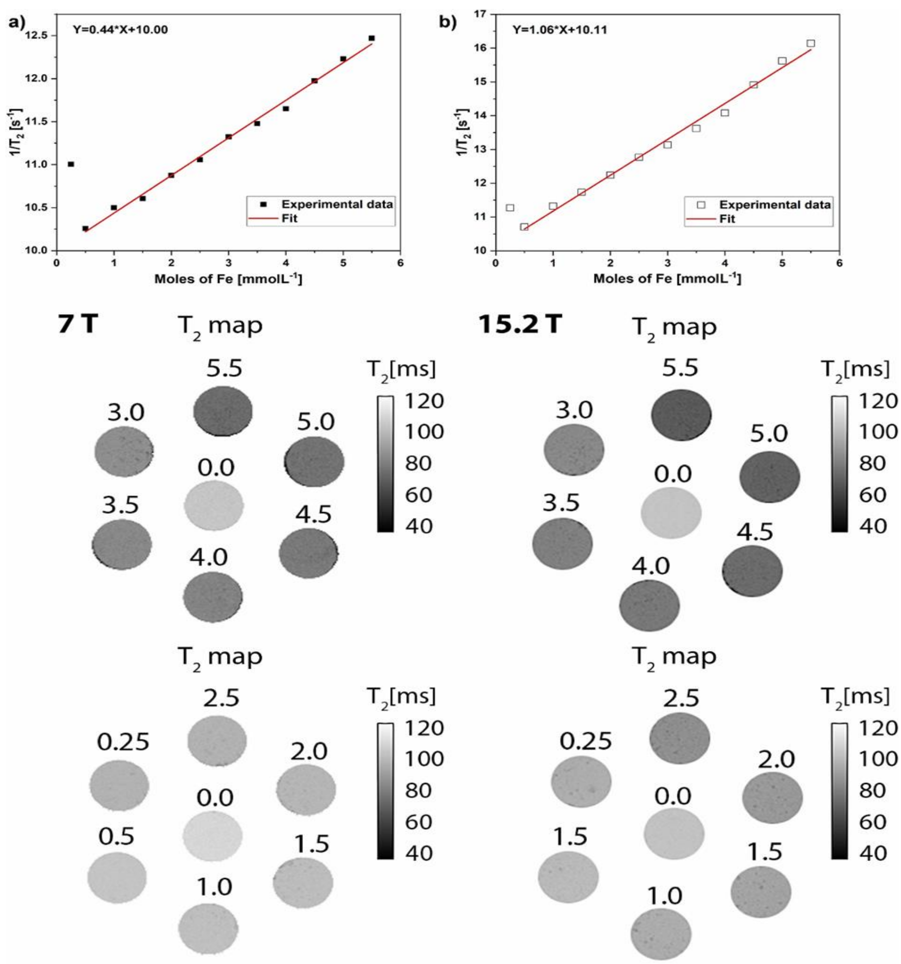

Figure 3 MRI relaxivity plots and T2 map of hematite NPs estimated at a) 7 T and b) 15.2 T (Tadic et al. 2022)

Tadic et al. (2021) in another paper synthesized a porous hematite/alumina magnetic nanocomposite by sol-gel synthesis technique and investigated its magnetic resonance imaging properties. They have reported the M(H) at 300 K exhibits coercivity (H_C) 293 Oe and magnetization (M_S) 2.71 emu/g and at 5 K 1150 Oe and 9.25 emu/g respectively. Such a promising magnetic property of the composite promotes it in MRI application. The transverse relaxivity rate (r2) of the nanocomposite show 0.44 mM^{-1} S^{-1} at 7 T and 1.06 mM^{-1} S^{-1} at 15.2 T (Tadic et al. 2022). Chen et al. (2021) synthesized cubical hematite nanoparticles and made a microrobot for macroblocks and impurities sweep. It has been demonstrated that in a low Reynolds number (Ra) environment, the microrobot was controlled by the vision-guided magnetic drive system in two different motion modes: rolling and tumbling. The microrobot was capable of tracking automatically generated predefined trajectories accurately and getting out from a micro-maze. The results showed that the microrobot has superior potential for biomedical sweep tasks in complex curved microchannels, similar to the blood vessels (Chen et al. 2021).

Naz et al. (2019) performed a phytomediated synthesis of rhombohedral hematite NPs from ferric chloride precursors with Rhus punjabensis as both a reducing and capping agent. The produced NPs' capacity to scavenge free radicals, their antioxidative potential, and their decreased power activities have all been demonstrated. The attachment of functional groups resembling flavonoids to the surface of nanoparticles causes these actions. Together with substantial antibacterial and antileishmanial activity, the NPs also inhibited protein kinase. NPs depicted a cytotoxic effect on DU-145 prostate cancer and HL-60 leukemic cell lines with 12.79 and 11.9 mg/ml of ED50 respectively (Naz et al. 2019).

CONCLUSION

The present article briefly introduces the different synthesis protocols of α-Fe_2O_3 (hematite) and its application in biomedical fields. Synthesis and application of nanomaterials are gaining the interest of the researcher last few decades. This article can help the researcher to gain knowledge about different synthesis protocols of such magnetic materials and their applications. Besides, this review will motivate researchers to explore different uses of hematite in biomedical fields.

REFERENCES

1. Banu, A. N., Kudesia, N., Raut, A. M., Pakrudheen, I., & Wahengbam, J. (2021). Toxicity, bioaccumulation, and transformation of silver nanoparticles in aqua biota: A review. Environmental Chemistry Letters, 19(6), 4275-4296
2. Mishra, S., & Singh, H. B. (2015). Biosynthesized silver nanoparticles as a nanoweapon against phytopathogens: exploring their scope and potential in agriculture. Applied microbiology and biotechnology, 99(3), 1097-1107
3. Vurro, M., Miguel-Rojas, C., & Pérez-de-Luque, A. (2019). Safe nanotechnologies for increasing the effectiveness of environmentally friendly natural agrochemicals. Pest management science, 75(9), 2403-2412
4. Muhammadi, Shabina, Afzal, M., & Hameed, S. (2015). Bacterial polyhydroxyalkanoates-eco-friendly next generation plastic: production, biocompatibility, biodegradation, physical properties and applications. Green Chemistry Letters and Reviews, 8(3-4), 56-77
5. Kim, H. J., Yim, E. C., Kim, J. H., Kim, S. J., Park, J. Y., & Oh, I. (2017). Bacterial nano-cellulose triboelectric nanogenerator. Nano Energy, 33, 130-137
6. Soufi, G. J., & Iravani, S. (2020). Eco-friendly and sustainable synthesis of biocompatible nanomaterials for diagnostic imaging: current challenges and future perspectives. Green Chemistry, 22(9), 2662-2687
7. Al-Hakkani, M. F., Gouda, G. A., & Hassan, S. H. (2021). A review of green methods for phyto-fabrication of hematite (α-Fe2O3) nanoparticles and their characterization, properties, and applications. Heliyon, 7(1), e05806
8. Dehner, C. A., Barton, L., Maurice, P. A., & DuBois, J. L. (2011). Size-dependent bioavailability of hematite (α-Fe2O3) nanoparticles to a common aerobic bacterium. Environmental science & technology, 45(3), 977-983
9. Rosso, K. M., Yanina, S. V., Gorski, C. A., Larese-Casanova, P., & Scherer, M. M. (2010). Connecting observations of hematite (α-Fe2O3) growth catalyzed by Fe (II). Environmental Science & Technology, 44(1), 61-67
10. Sharma, P., Dhiman, S., Kumari, S., Rawat, P., Srivastava, C., Sato, H., Akitsu, T., Kumar, S., Hassan, I. & Majumder, S. (2019). Revisiting the physiochemical properties of Hematite (α-Fe2O3) nanoparticle and exploring its bio-environmental application. Materials Research Express, 6(9), p.095072
11. Momeni, M.M., Ghayeb, Y. & Mohammadi, F. (2015). Solar water splitting for hydrogen production with Fe2O3 nanotubes prepared by anodizing method: effect of anodizing time on performance of Fe2O3 nanotube arrays. Journal of Materials Science: Materials in Electronics, 26(2), 685-692
12. Momeni, M. M., Ghayeb, Y., & Mohammadi, F. (2015). Fe2O3 nanotube films prepared by anodisation as visible light photocatalytic. Surface Engineering, 31(6), 452-457
13. Tadic, M., Kopanja, L., Panjan, M., Lazovic, J., Tadic, B.V., Stanojevic, B., & Motte, L. (2021). Rhombohedron and plate-like hematite (α-Fe2O3) nanoparticles: Synthesis, structure, morphology, magnetic properties and potential biomedical applications for MRI. Materials Research Bulletin, 133, p.111055
14. Paulson, E., & Jothibas, M. (2021). Significance of thermal interfacing in hematite (α-Fe2O3) nanoparticles synthesized by sol-gel method and its characteristics properties. Surfaces and Interfaces, 26, 101432
15. Eid, C., Luneau, D., Salles, V., Asmar, R., Monteil, Y., Khoury, A., & Brioude, A. (2011). Magnetic properties of hematite nanotubes elaborated by electrospinning process. The Journal of Physical Chemistry C, 115(36), pp.17643-17646
16. Eid, C., Brioude, A., Salles, V., Plenet, J. C., Asmar, R., Monteil, Y., … & Miele, P. (2010). Iron-based 1D nanostructures by electrospinning process. Nanotechnology, 21(12), 125701 Trpkov, D., Panjan, M., Kopanja, L., & Tadić, M. (2018).
17. Hydrothermal synthesis, morphology, magnetic properties and self-assembly of hierarchical α-Fe2O3 (hematite) mushroom-, cube-and sphere-like superstructures. Applied Surface Science, 457, 427-438
18. Zhu, M., Wang, Y., Meng, D., Qin, X., & Diao, G. (2012). Hydrothermal synthesis of hematite nanoparticles and their electrochemical properties. The Journal of Physical Chemistry C, 116(30), 16276-16285
19. Ghosh, S., Roy, S., Bardhan, S., Khatua, N., Bhowal, B., Chanda, D.K., Das, S., Mondal, D., Basu, R., & Das, S. (2021). Effect of size fractionation on purity, thermal stability and electrical properties of natural hematite. Journal of Electronic Materials, 50(7), 3836-3845
20. Wang, W., Howe, J. Y., & Gu, B. (2008). Structure and morphology evolution of hematite (α-Fe2O3) nanoparticles in forced hydrolysis of ferric chloride. The Journal of Physical chemistry C, 112(25), 9203-9208
21. Liu, G., Deng, Q., Wang, H., Ng, D. H., Kong, M., Cai, W., & Wang, G. (2012). Micro/nanostructured α-Fe2O3 spheres: synthesis, characterization, and structurally enhanced visible-light photocatalytic activity. Journal of Materials Chemistry, 22(19), 9704-9713

22. Liu, Q., Barrón, V., Torrent, J., Qin, H., & Yu, Y. (2010). The magnetism of micro-sized hematite explained. Physics of the Earth and Planetary Interiors, 183(3-4), 387-397.
23. Chen, Y. H., & Lin, C. C. (2014). Effect of nano-hematite morphology on photocatalytic activity. Physics and Chemistry of Minerals, 41, 727-736
24. Zhao, J., Yang, P., Chen, H. S., Li, J., Che, Q., Zhu, Y., & Shi, R. (2015). Effect of sequential morphology adjustment of hematite nanoplates to nanospindles on their properties and applications. Journal of Materials Chemistry C, 3(11), 2539-2547
25. Zhu, M., Wang, Y., Meng, D., Qin, X., & Diao, G. (2012). Hydrothermal synthesis of hematite nanoparticles and their electrochemical properties. The Journal of Physical Chemistry C, 116(30), 16276-16285
26. Chen, Y. H., & Lin, C. C. (2014). Effect of nano-hematite morphology on photocatalytic activity. Physics and Chemistry of Minerals, 41, 727-736.
27. Dena, A. S. A., Abdelaziz, O. A., & El-Sherbiny, I. M. (2022). Nanomaterials: classification, composition, and recent advances in synthesis. Immunomodulatory Effects of Nanomaterials, 1-19
28. Dahl, J.A., Maddux, B.L. & Hutchison, J.E. (2007). Toward greener nanosynthesis. Chemical reviews, 107(6), 2228-2269
29. Gutfleisch, O., Willard, M.A., Brück, E., Chen, C.H., Sankar, S.G. & Liu, J.P. (2011). Magnetic materials and devices for the21st century: stronger, lighter, and more energy efficient. Advanced materials, 23(7), 821-842
30. Smith, B. D., Mayer, T. S., & Keating, C. D. (2012). Deterministic assembly of functional nanostructures using nonuniform electric fields. Annual review of physical chemistry, 63, pp.241-263
31. Strano, V., Greco, M. G., Ciliberto, E., & Mirabella, S. (2019). ZnO Microflowers Grown by Chemical Bath Deposition: A Low-Cost Approach for Massive Production of Functional Nanostructures. Chemosensors, 7(4), p.62
32. Othman, A., Karimi, A., & Andreescu, S. (2016). Functional nanostructures for enzyme based biosensors: Properties, fabrication and applications. Journal of Materials Chemistry B, 4(45), 7178-7203
33. Li, Z., Dong, K., Huang, S., Ju, E., Liu, Z., Yin, M., Ren, J., & Qu, X. (2014). A smart nanoassembly for multistage targeted drug delivery and magnetic resonance imaging. Advanced Functional Materials, 24(23), 3612-3620
34. Ma, X., Tao, H., Yang, K., Feng, L., Cheng, L., Shi, X., Li, Y., Guo, L., & Liu, Z. (2012). A functionalized graphene oxide-iron oxide nanocomposite for magnetically targeted drug delivery, photothermal therapy, and magnetic resonance imaging. Nano Research, 5(3), 199-212
35. Nakamura, T., Sugihara, F., Matsushita, H., Yoshioka, Y., Mizukami, S., & Kikuchi, K. (2015). Mesoporous silica nanoparticles for 19 F magnetic resonance imaging, fluorescence imaging, and drug delivery. Chemical science, 6(3), 1986-1990
36. Liu, C., Chen, H., Zhou, H., Yu, S., Wang, N., Yao, W., Lu, A. H., & Qiao, W. (2021). Magnetic Resonance Imaging-Guided Multi-Stimulus-Responsive Drug Delivery Strategy for Personalized and Precise Cancer Treatment. ACS Applied Materials & Interfaces, 13(43), 50716-50732
37. Tadic, M., Panjan, M., Tadic, B.V., Kralj, S., & Lazovic, J. (2022). Magnetic properties of mesoporous hematite/alumina nanocomposite and evaluation for biomedical applications. Ceramics International, 48(7), pp.10004-10014
38. Chen, W., Fan, X., Sun, M., & Xie, H. (2021). The cube-shaped hematite microrobot for biomedical application. Mechatronics, 74, p.102498
39. Naz, S., Islam, M., Tabassum, S., Fernandes, N. F., de Blanco, E. J. C., & Zia, M. (2019). Green synthesis of hematite (α-Fe2O3) nanoparticles using Rhus punjabensis extract and their biomedical prospect in pathogenic diseases and cancer. Journal of Molecular Structure, 1185, 1-7

Acknowledgments

The authors would like to acknowledge the Dept. of Physics, Jadavpur University, India, and D.M and S.D would like to thank the UGC-DAE-CSR scheme (CRS/2021-22/02/498) for funding.